Kyle E. Brown
Department of Physics,
Arizona State University,
Tempe, AZ 85281
e-mail: kebrow17@asu.edu

Amir Baniassadi
School of Sustainable Engineering and the Built Environment,
Arizona State University,
Tempe, AZ 85281;
Graduate School of Design,
Harvard University,
Cambridge, MA 02138
e-mail: abaniassadi@gsd.harvard.edu

Julie V. Pham
School for Engineering of Matter, Transport and Energy,
Arizona State University,
Tempe, AZ 85281
e-mail: jvpham1@asu.edu

David J. Sailor[1]
School of Geographical Sciences and Urban Planning,
Arizona State University,
Tempe, AZ 85381
e-mail: david.sailor@asu.edu

Patrick E. Phelan
School for Engineering of Matter, Transport and Energy,
Arizona State University,
Tempe, AZ 85287
e-mail: phelan@asu.edu

Effects of Rooftop Photovoltaics on Building Cooling Demand and Sensible Heat Flux Into the Environment for an Installation on a White Roof

Photovoltaic (PV) panels are commonly used for on-site generation of electricity in urban environments, specifically on rooftops. However, their implementation on rooftops poses potential (positive and negative) impacts on the heating and cooling energy demand of buildings, and on the surrounding urban climate. The adverse consequences can be compounded if PV is installed on top of an otherwise highly reflective ("white") rooftop. This study investigates these impacts on a test building in Tempe, AZ, by directly measuring the temperature of all involved surfaces. These measurements are supplemented by whole-building energy simulations to model the energy implications for archetypical residential and retail buildings. This includes calculations of the ratio of the energy demand penalty to electricity generation as well as the net sensible heat flux to the ambient environment. Results indicate that the summertime cooling energy penalty due to blockage of outgoing longwave radiation can be 4.9—11.2% of the PV electricity generation. The addition of PV to the white roof resulted in a small decrease in the computed sensible heat flux at night, but a daytime increase in sensible flux by more than a factor of 10 (from less than 25 W/m^2 for the white roof alone, to more than 250 W/m^2 when PV is added to the roof). This study highlights the potential unintended consequences of rooftop PV under certain conditions and provides a broader perspective for building designers and urban planners.
[DOI: 10.1115/1.4046399]

Keywords: air conditioning, building, cities, clean energy, energy, environment, photovoltaics

1 Introduction

The global climate is approaching a tipping point as the global temperature rises. According to the Intergovernmental Panel on Climate Change's 2018 report, extreme global consequences will likely arise after temperatures increase by 1.5 °C [1]. Greenhouse gases (and carbon dioxide, in particular) are identified as the root cause of anthropogenic climate change and fossil fuels are the principal contributor of CO_2 emissions [2]. Furthermore, dependence on fossil fuels causes energy insecurity [3], injustice [4], and emission of a variety of pollutants other than CO_2. Thus, transitioning to renewable and low-carbon energy sources is a pressing need. Currently, utility scale renewables such as hydroelectric dams, wind farms, solar farms, etc. are dominant in terms of total installed renewable capacity in the United States. However, one issue with utility scale generation is the lack of diversity in land use. These single-use lands are often far from population hubs, leading to higher transmission losses. The other type of renewable energy system is distributed energy resources (DER), where the generation takes place on a small scale in proximity to the loads. As the user is closer to the site of generation, the electricity transmission losses are reduced [5]. The installation of PV panels in cities on widely underutilized rooftop spaces is an example of DER [6].

Despite numerous benefits, there are potential negative impacts from rooftop PV implementation. Currently installed photovoltaic panels typically convert only 15–18% of the incoming solar radiation into electricity [7]. As a result, most of the incident radiation is absorbed into the panel as heat and released into the urban environment. Little research has been conducted on the effects of PV panels on the urban climates. The majority of papers in the literature states that PV systems have no effect or a beneficial effect on the urban heat island [8–12]. This view may come from a lack of consideration of the effects of long wave radiation trapping as well as the number of surfaces (top and bottom) that contribute to convective heat loss from PV panels. On the other hand, there are a few studies that show an urban warming effect. For example, Pham et al. [13] reported that photovoltaics can increase the sensible heat flux by 80% when compared with unshaded asphalt and the effect would be exacerbated compared with a white shade surface [13]. In addition, Scherba et al. [14] reported that in the case of PV panels on top of a white roof, a net warming of the urban climate can be expected.

There is also not a clear consensus on the impact of rooftop PV panels on building heating and cooling loads. The majority of studies suggest that rooftop PV arrays provide beneficial shading to the building and reduce cooling loads [15–19]. However, some state that the only PV panels that provide a cooling benefit are those on roofs that initially had a low reflectivity in the shortwave spectrum (albedo) or were flush mounted [16,17]. Multiple studies that claim PV roofs yield a reduction in cooling loads generally focus testing on conventional, low albedo roofs [18,19]. However, the effects of PV on a high-albedo roof may provide differing results. Dominguez et al. [15] used a high-albedo rooftop in their experiment; however, the tested building lacked indoor

[1]Corresponding author.

Manuscript received September 23, 2019; final manuscript received February 12, 2020; published online February 19, 2020. Assoc. Editor: Shiguang Miao.

temperature control, which makes the results inapplicable to most building types. Another common limitation of past studies is the focus on a single day of data [15,18]. Given that these impacts are sensitive to weather parameters, it is not possible to generalize their findings to all conditions.

To address these issues and expand upon the literature, we investigated the thermal impacts of rooftop PV arrays on the urban climate as well as on building energy loads when applied on top of a high-albedo roof. This study analyzed a data set from 2 months of continuous measurement of variables necessary to calculate sensible heat flux as well as modeling cooling energy demand of the building. In addition, to understand the relationship of panel height to cooling loads, two separate array heights were tested. In EnergyPlus, the collected data are used to model residential and commercial scale buildings at each array height, and the energy losses are compared with the PV electricity generation.

2 Materials and Methods

We constructed a test PV array of nine panels and installed it on a test building with a flat, white roof. Data were collected for August and September of 2018. Sensors logged temperatures on the underside surface of the center PV panel and both the inside and outside of the roof at two locations: underneath the center of the PV array and on the unshaded part of the roof.

2.1 Test Building. The test building (Fig. 1) is of dimensions 2.44 m × 2.44 m × 2.44 m and is located in Tempe, AZ on the roof of Design North Building on Arizona State University's Tempe Campus (33.421564, −111.937255). The building has a wood-frame construction with a flat roof and two double-paned, aluminum framed windows of dimension 80 cm by 49 cm on its south, west, and east walls. The north-facing wall has a single window fitted with a 600-W air conditioning unit. The air conditioning set point was at a constant 27 °C. Two large box fans were run in the space to ensure uniformity of indoor air temperatures within the test structure.

2.2 Scale Model Solar Array. The scale model rooftop photovoltaic array (Fig. 2) consisted of nine 5-W panels (Solarland SLP005-12U), with dimensions of 22.2 cm by 27 cm by 1.8 cm, in a 3 by 3 array. The tilt angle is 8 deg, typical of installations in the region. The height of the array, measured at the center of the panels, was varied between 10 and 28 cm (henceforth, H-10 and H-28) above the roof surface.

2.3 Surface Albedo Measurements. We measured the reflectance of the PV panel and roof surface using a field spectrometer (Analytical Spectral Devices FieldSpec 4 with a stated accuracy of ±2%). The spectrometer was calibrated using a 99% reflectance standard prior to measuring the reflectance of each surface. The albedo was calculated by averaging the reflectance of 10 trials for each surface and then multiplying by the ASTM G173 global irradiance standard [20] to arrive at spectral reflectance (Fig. 3). The albedo was determined to be 0.11 for the PV panel and 0.63 for the reflective (white) roof.

2.4 Data Collection. Measurements were taken during August and September of 2018, alternating (weekly) between the H-10 and H-28 settings. On the roof of the building, surface temperature was measured with thermocouples (OMEGA Self-adhesive thermocouple, Type E, accurate to ±0.3 °C). The sensors measured the underside temperatures of the central panel, and both sides of the roof at two locations as shown in Fig. 4 (a total of five sensors). This location was approximately 0.5 m from the edge of the building roof, which was helpful in minimizing edge effects of upwelling radiation from the nearby surroundings and horizontal conduction effects within the roof itself.

In addition, the current and voltage of the center panel was measured using Omega current and voltage sensors (5 μA resolution, ±0.05% full scale range for current logger and 0.5 mV resolution ±0.05% calibrated accuracy for voltage). Each panel was connected to a single (remotely located) resistor (10 Watt, 150 Ohm, 5% tolerance) to act as a load. Throughout the course of each day, the roof surface temperature on the high-albedo roof was never shaded by the array or any other surrounding structures. Inside of the test building, two thermocouples were adhered to the ceiling using conductive tape, one directly underneath the panel array and one underneath the white roof. Data from all sensors were logged using a Campbell Scientific CR1000 data logger in intervals of 1 minute, with synchronized initiation time. The indoor air temperature was monitored by two Kestrel Drop loggers (thermistors) hung from the ceiling to ensure that indoor temperatures remain consistent. The indoor air temperature was measured in intervals of 30 min. The weather data were provided by a weather station located 10 km to the Northwest of the study site (33.457479, −112.040167) for ambient temperature, global radiation, and wind velocity. The average minimum and maximum temperatures during the test period were 27 and 41 °C. The (24-h) average solar radiation for the period was 265W/m^2. The weather station at Sky Harbor International Airport (Phoenix Skyharbor Airport) provided weather data for cloud cover, relative humidity,

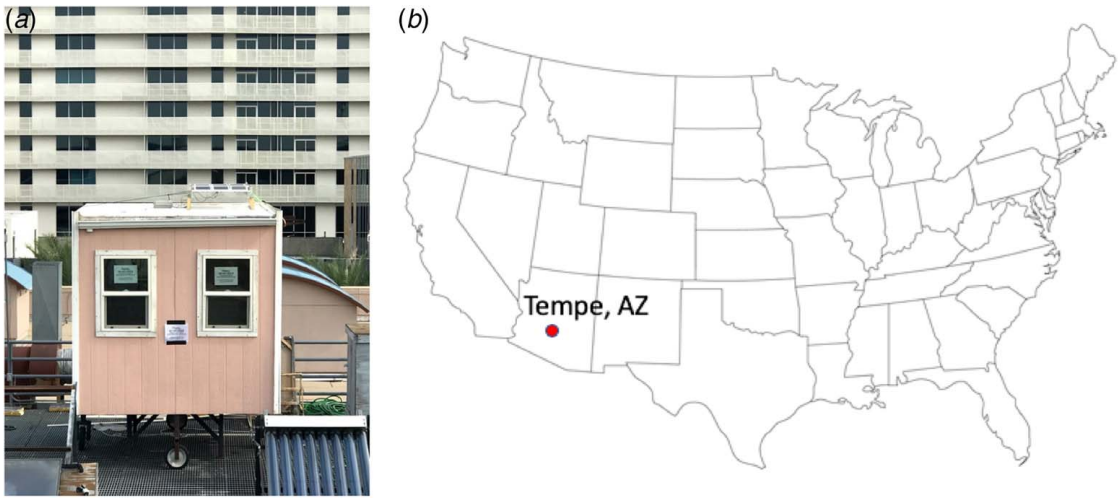

Fig. 1 (*a*) Image of the test building on the roof of the Design North Building on Arizona State University's Tempe campus and (*b*) general location in the desert southwest of the U.S.

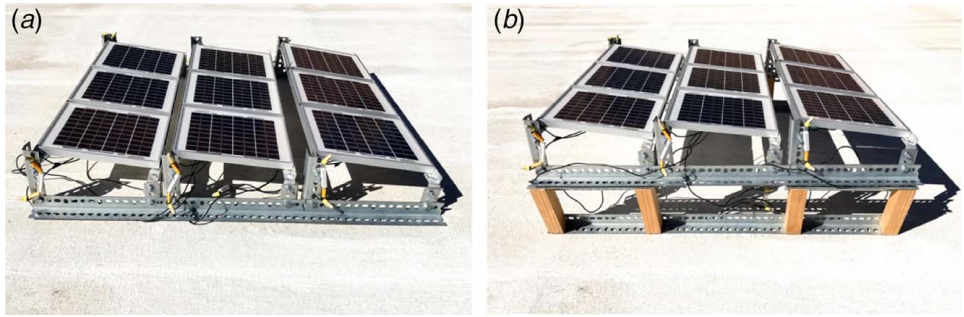

Fig. 2 PV array apparatus installed on the roof of the test building (*a*) H-10 and (*b*) H-28

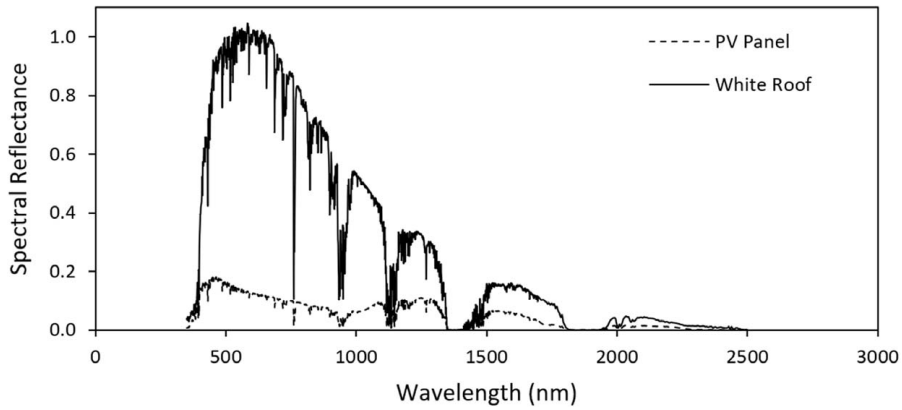

Fig. 3 Spectral reflectance of PV and white roof surfaces during a typical, clear August day in Tempe, AZ

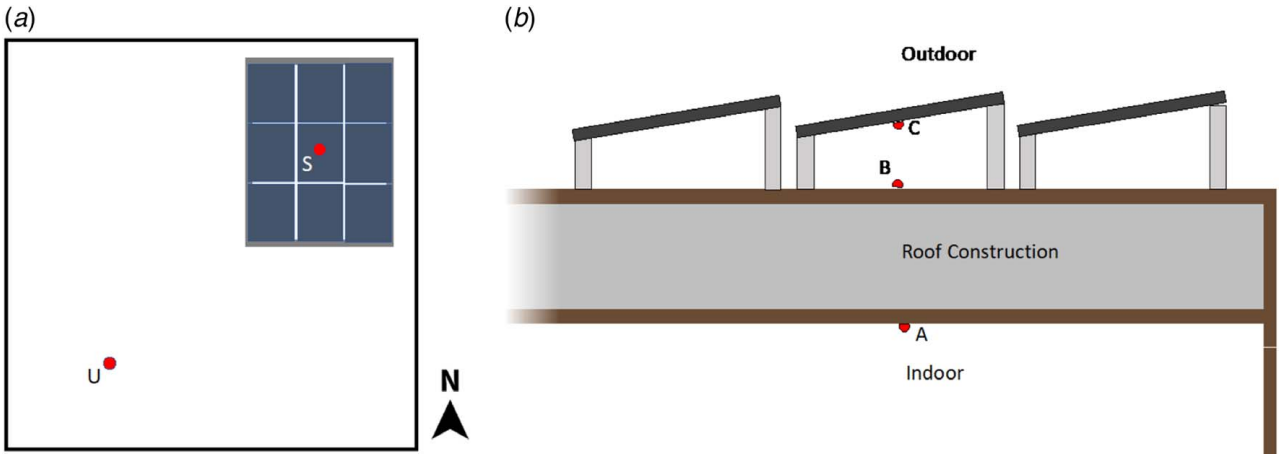

Fig. 4 (*a*) Schematic of sensor installation locations in relation to the roof layout. Point U is the location of the unshaded white roof case and point S is the location of the case shaded by the PV array. (*b*) Schematic of sensor installation locations in relation to the PV panels. Point A is the location of the shaded ceiling surface temperature, point B is the location of the shaded roof surface temperature, and point C is the location of the panel surface temperature.

and dew point temperature. A filtering procedure was used to eliminate outliers in the data. For daytime (9:00 a.m.–5:00 p.m.), we conducted a rank and percentile analysis of the solar radiation and wind speed. Days in the bottom 10% of mean daily solar radiation and top 10% of mean daily wind speed were filtered out. For nighttime (9:00 p.m.–5:00 a.m.), we repeated the same procedure while replacing solar radiation with cloud cover. Nights in the top 10% of both cloud cover and wind speed were filtered out. Then, we excluded all dates eliminated in either the day or night filtering (17 total) from the measurement period. Finally, the data for the entire day was used to develop an average diurnal profile for each PV array height case (H-10 and H-28).

2.5 Whole-Building Energy Simulations

2.5.1 EnergyPlus. To assess the end-point impacts of rooftop PV on energy consumption of actual buildings with realistic loads, we relied on whole-building energy models of archetypical residential (a single-family detached unit) and commercial (a single-story retail store) buildings. In this study, we used

EnergyPlus, a tool developed and validated by U.S. Department of Energy [21,22], to conduct the building simulations. We ran our simulation by forcing the building models with outdoor weather variables from the same sources and for the same average diurnal profile we described in Sec. 2.4. The simulations that included PV arrays were run assuming the array covered 100% of the rooftop area.

2.5.2 Model Buildings. The residential archetype was a 110 m^2 single-family residential building, the most common residential building type in Phoenix [23,24]. We set all input parameters (except the rooftop) in compliance with Building America House Simulation Protocol [25], a methodology developed by the National Renewable Energy Laboratory to standardize modeling of energy-saving strategies in residential buildings. With the exception of roof thermal insulation (e.g., R-value), all other regulated envelope and system characteristics comply with the 2003 version of the International Energy Conservation Code. Similar to typical buildings in Phoenix, cooling in the modeled building is provided by a direct expansion central air conditioning unit. The commercial building model was directly downloaded from the set developed and made publicly available by the U.S. Department of Energy. From this "Commercial Prototype Building Models" set, we selected the "Stand-alone Retail" archetype compliant to ASHRAE standard 90.1 2004. The footprint of the retail building is 2279 m^2. The code selection for both archetypes was based on the status of energy code implementation [26] in Arizona and represents buildings built in the 21st century. Figure 5 shows the outline of both building models.

2.5.3 Implementing the Rooftop PV in EnergyPlus. EnergyPlus is capable of modeling PV performance and the impact of their shade on exterior building surfaces [27]. However, similar to other building energy simulators, an important limitation in the current version (V8.8) of the EnergyPlus rooftop PV model is the exclusion of longwave radiation between the shaded roof and the panels [14,28]. While EnergyPlus accounts for the shade from incoming shortwave radiation, it does not consider the fact that (potentially hot) PV panels impede longwave radiative heat exchange between the roof and the sky. Therefore, researchers (who are cognizant of this shortcoming) rely on other methods to mimic these effects. For example, Peng and Yang [28] set the air gap between the panels and the roof as a non-conditioned thermal zone. However, they acknowledged that this approach is only reliable when the gap size is small and has limited ventilation. Scherba et al. [14] took a different approach and modified the weather file. By changing the sky temperatures, they effectively replaced the "sky" object with the "panels." In this study, we took another approach and completely bypassed the roof energy balance model by forcing the measured outside surface temperature time-series into the model. First, we used a combination of measured inside and outside roof surface temperature and indoor air temperature data to derive the overall heat transfer coefficient of the roof and the inside surface convective coefficient. We ran parametric simulations in EnergyPlus to find the set of values that result in minimum error in predicting the surface temperature of the inside of the roof while forcing the model with measured outside surface temperature and indoor air temperature. The best fit (RSME = 0.3 °C) was obtained with a roof thermal insulation R-value of 2.2 m^2·K/W (12.6 ft^2·°F·h/BTU)—which was in line with our own estimates based on the existing material—and an indoor surface convection coefficient of 20 W/m^2 K. Since both mixing fans were continuously working at the same speed and direction, we assumed that the indoor convective heat transfer coefficient is constant throughout the day. Then, we implemented the same roof object in the archetype buildings and used the model thermostat set point equal to the set point in the test building. Excluding the inside roof surface temperature, all other components of the building cooling load are dynamically solved for by EnergyPlus in response to outdoor weather conditions and occupancy schedules. The advantage of this approach is that it does not require any modeling assumption as it forces the model with measured data from the rooftop. However, the limitation is that it can only be used for the scenario for which detailed measured data are available, and thus cannot be relied upon for exploring other configurations.

2.6 Sensible Heat Flux Calculations. Calculations of the sensible heat flux used measurements of surface temperature, local wind speed, tilt angle, roughness coefficients, and ambient dry bulb temperature. The model for convective (sensible) heat flux is based on the algorithm first used in DOE-2 software [29]. Equation (1) calculates sensible heat flux, q_c, and is evaluated for both sides of PV panels as well as the roof surfaces

$$q_c = h_c \times (T_s - T_a) \tag{1}$$

In this equation, q_c is the sensible heat flux, T_s (°C) represents the surface temperature of each surface, and T_a (°C) represents the ambient dry bulb air temperature. The top and bottom surface temperatures are approximated to be the same due to the negligible thermal mass of the PV panel. The reference air temperature is assumed to be the same above and below the panel. This assumption is generally reasonable for larger vertical spacing between the panel and the roof surface. However, the air temperature between the panel and roof can be substantially warmer than The heat transfer coefficient, h_c, is calculated for upward- and downward-facing surfaces using the following:

$$h_c = h_n + R_f(h_{c0} - h_n) \tag{2}$$

$$h_{c0} = \sqrt{h_n^2 + (aV^b)^2} \tag{3}$$

where h_{c0} is the film heat transfer coefficient and R_f, a, and b are experimental coefficients all derived from the work of Yazdanian and Klems [30]). V(m/s) is the local wind speed and h_n is the natural convection coefficient. The natural convection coefficient for the upward (roof and PV) and downward (PV) facing

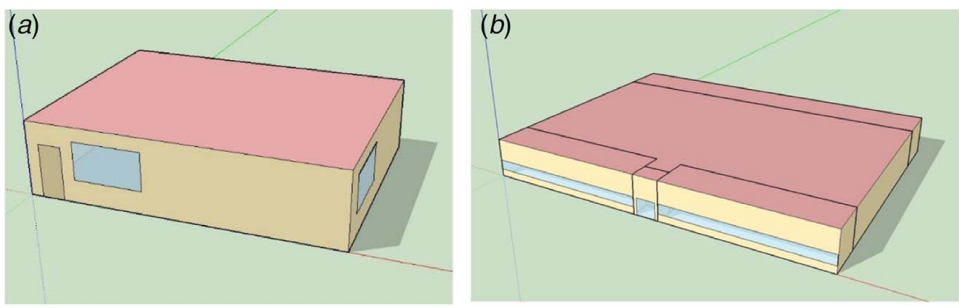

Fig. 5 Model building outlines: (*a*) residential archetype and (*b*) retail archetype

surfaces of the system are calculated using the following pair of equations [29]:

$$h_n = \frac{9.842 \times |\Delta T|^{1/3}}{7.283 - |\cos\theta|} \quad \text{(upward)} \tag{4}$$

$$h_n = \frac{1.810 \times |\Delta T|^{1/3}}{1.382 + |\cos\theta|} \quad \text{(downward)} \tag{5}$$

In both, ΔT (°C) is the temperature difference between the ambient and surface and θ is the tilt angle of the panel. The final calculations found the sensible heat flux to the urban environment for the two heights (H-10 and H-28) of the PV array, as well as the white roof. For the case of the PV panels, the total flux was the sum of both sides of the panel and the shaded portion of roof below it.

3 Results and Discussion

In addition to estimating the sensible heat flux into the environment, we calculated total electric energy generation and cooling energy costs associated with the complex radiation balance on rooftop PVs.

3.1 Impacts on the Urban Environment

3.1.1 Outdoor Surface Temperatures. Figure 6 presents hourly profiles (average diurnal profile) of surface–air temperature differences for the shaded and unshaded roof as well as for the PV panel surface. The left-hand panel is for the lower of the two panel heights (H-10) and the right-hand panel is for the H-28 height.

One notable characteristic of this plot is that the unshaded roof surface reaches a higher temperature than the shaded roof surface only during the 9 a.m.–3 p.m. window. For the remainder of the time, the difference in temperature between the PV roof surface and the white roof surface at night is nearly constant with the shaded roof being the hotter surface. This is true for both of the height cases, although during the peak of the day, the difference between PV and roof surface temperatures is three times larger in the H-28 case. This can be explained by considering that there is a near tripling of the heights of the panels which significantly increases the sky view factor of the roof surface underneath the panels. As a result, the longwave emission from the H10 case is more effective at warming the roof surface. Thus, the peak temperature is not as affected by the peak radiation. One apparent anomaly in this figure is that, for the H-28 scenario, the shaded roof surface reveals modest peaks in surface temperature in mid-morning and mid-afternoon hours. This is likely a result of direct solar radiation reaching the area of the thermocouple measurement at low sun angles. Such peaks would not be present in a larger array of panels.

3.1.2 Sensible Heat Flux Into the Urban Environment. The total rooftop daily sensible heat fluxes (as calculated from Eq. (1)) into the urban environment were calculated (Fig. 7) in order to explore the impact of the PV installations on the urban climate. The daytime window for analysis was defined as from 9:00 a.m. to 5:00 p.m. and the nighttime window is from 9:00 p.m. to 5:00 a.m. The daytime flux from the PV panels is 12–13 times higher than that of the unshaded white roof. The daytime H-28 sensible flux was 8% lower than that of the H-10 case. At night, there is a consistent negative heat flux across all cases; however, the white roof flux was three times larger than both of the PV cases. Of course, sensible fluxes at night are much lower than during the day. Hence, it is useful to consider 24-hour averages. Over the course of an average day the flux to the urban environment is positive for both PV cases whereas the flux for the white roof was negative. Furthermore, the PV cases are responsible for contributing a daily average of 130–140 W/m^2 more heat flux into the urban environment during an entire summer day compared with the white roof case. As the albedo of the white roof in this study is 0.63, it is typical of a weathered white roof (e.g., [31]). These findings are consistent with the results of Scherba et al. [14] who found that the addition of PV panels to a white roof will increase the sensible heat flux. This increase in sensible heat flux from building rooftops will be in addition to the atmospheric warming effects associated with air conditioning waste heat, exfiltration, and sensible heating from other facades of buildings (e.g., [32,33]).

3.2 Energy Implications. As seen in the results for temperature differences and sensible heat flux, PV panels make the rooftops hotter. We conducted simulations to understand how this surface temperature increase impacts the cooling energy demand of the building. The simulations covered four different cases, the residential and retail archetypes at PV heights of H-10 and H-28. The simulations calculated the amount of cooling load increase for each case compared with the white roof case. Figure 8 shows the difference in the gross and net generation of the PV panels when accounting for the increased cooling loads. This is calculated for the full day as well as the for the peak hours of the utility company serving the region (Arizona Public Service), which is 3:00 p.m. to 8:00 p.m.

As is clear from these results, the addition of rooftop PV increases the overall cooling loads and thereby decreases the net generation of the array by at least 5%. At its highest impact, there is more than an 11% penalty associated with increased cooling demand (H-10, retail case). This shows that while the PV array may still generate usable energy, its addition does cause an increase in energy demand for cooling the building. It is notable that the H-28 height generally had a smaller impact on cooling load, which is likely due to a combination of increased sky view factor for long wave radiative exchange, and improved air flow for

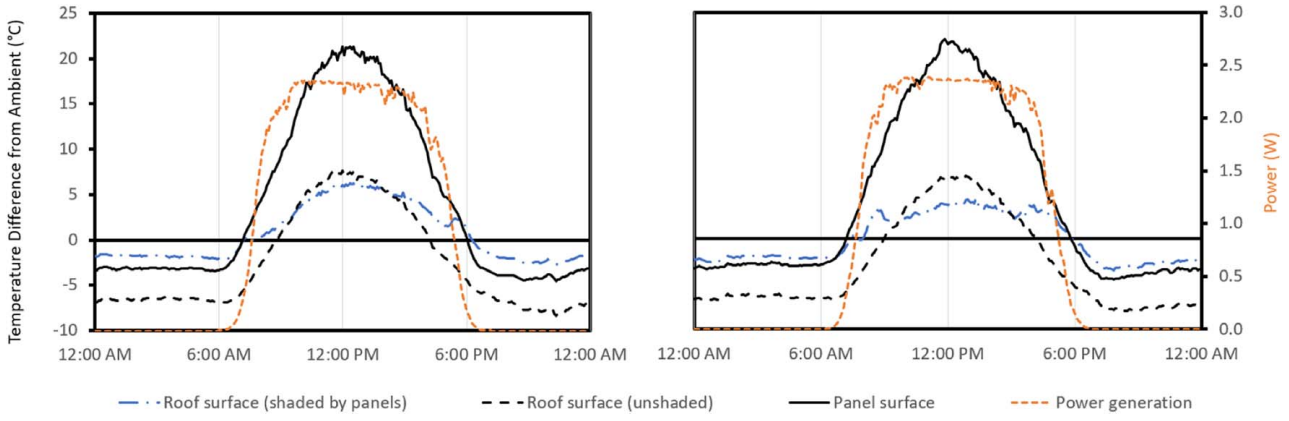

Fig. 6 Average diurnal profiles of outdoor surface temperature difference from ambient and panel generation

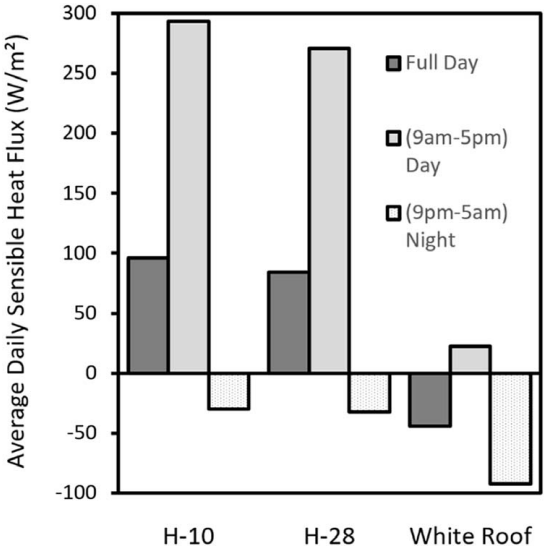

Fig. 7 Average daily sensible heat flux into the urban environment (sum for all surfaces) for a representative day

convective cooling of the panels and roof. The exception is the retail archetype during peak hours, where H-28 had a slightly larger impact on the cooling load. Also, PV installed on the retail archetype consistently resulted in larger impacts on cooling loads compared with the retail case. This might be attributable to the higher occupancy during hours of peak insolation, resulting in a larger air conditioning penalty for the retail cases. While we highlight these implications, we note that even with a relatively clean energy mix, rooftop PVs reduce the total carbon emissions. However, our results show that without considering the thermal interactions between the building and the urban environment, the net carbon (and cost) benefits of rooftop PV might be overestimated.

4 Conclusions

Analysis of data from a PV array installed on a white roof in Tempe, AZ has shown that both sensible heat fluxes and cooling loads increase during summer months. The results revealed that when compared with a reflective white roof alone, the addition of PV panels causes more than a 10-fold increase in daytime sensible heat flux to the urban environment. Whole-building energy simulations of archetype buildings revealed that the addition of PV panels can cause an air conditioning energy penalty and that this penalty is larger for retail buildings than for residential buildings. The increase in cooling load is considerably higher for panels with a lower height above the roof surface. Specifically, for the case of the 10 cm PV height above the roof, the resulting increase in cooling loads was equivalent to 11% of the total electricity generation from the panels. Overall, this study illustrates that PV arrays do heat the urban environment, as well as increase the cooling loads of the attached building. Without considering these factors, the net benefit of PV panels might be overestimated. Therefore, they need to be considered in decision processes related to implementation of PV.

As the present study focused on one location, measurements for a single test building, and on simulations for only two archetypes, it is difficult to draw broad conclusions for the building stock as a whole. Certainly, the results would differ for buildings with stronger/weaker thermal coupling between the roof and the building interior (e.g., less/more insulation). Also, the PV panels tested in this study had relatively low efficiency of 12%. Panels are currently commercially available with efficiencies in the 16–20% range. The results for panels with higher efficiencies would clearly lead to less of a heating impact on the urban climate. There would also likely be a modest reduction in the air conditioning energy penalty as higher efficiency panels would run cooler, radiating less long wave energy to the building during the day. This clearly points to an opportunity for future research and development work to develop panels and installation practices that minimize these adverse effects of rooftop PV.

While there is certainly room for follow-on studies to address limitations and add detail to the results presented here, this study is fairly unambiguous in its findings that rooftop PV warms the

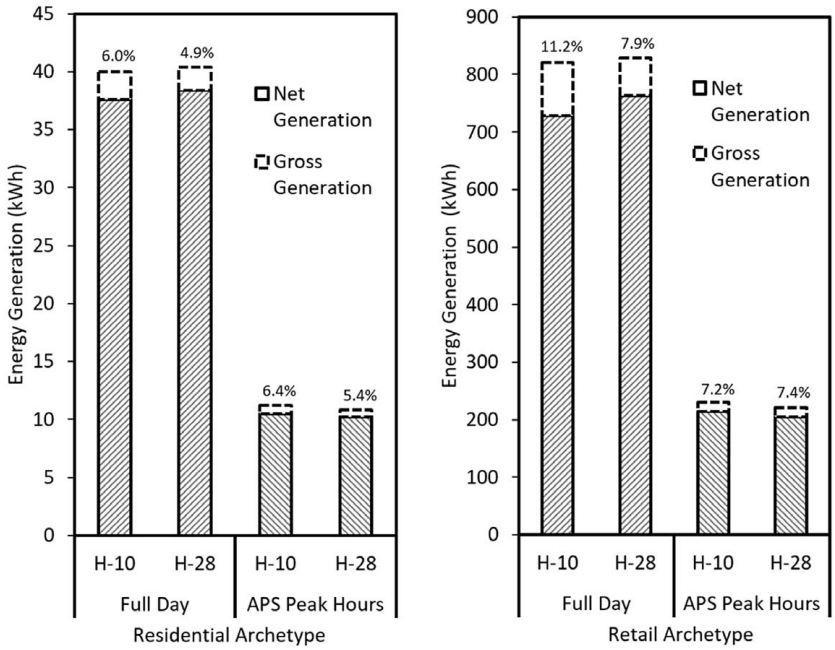

Fig. 8 Net and gross energy generation for the four different cases in full day and Arizona Public Service (local utility) peak hours. The percentages represent the percent increase in cooling loads compared with the gross generation.

urban environment while also causing a modest air conditioning energy use penalty.

Acknowledgment

The authors wish to acknowledge support from the Urban Climate Research Center, Design School and Barrett, and the Honors College of Arizona State University. The authors also wish to acknowledge funding support from the Urban Climate Research Center, the Barrett Honors College at Arizona State University, and the Fulton/GORE student program. This work was also supported in part by the National Science Foundation under grant number 1623948.

Conflicts of Interest

None.

References

[1] IPCC, 2018, Global Warming of 1.5°C. An IPCC Special Report on the impacts of global warming of 1.5°C above pre-industrial levels and related global greenhouse gas emission pathways, in the context of strengthening the global response to the threat of climate change, sustainable development, and efforts to eradicate poverty [Masson-Delmotte, V., Zhai, P., Pörtner, H.-O., Roberts, D., Skea, J., Shukla, P.R., Pirani, A., Moufouma-Okia, W., Péan, C., Pidcock, R., Connors, S., Matthews, J.B.R., Chen, Y., Zhou, X., Gomis, M. I., Lonnoy, E., Maycock, T., Tignor, M., and Waterfield, T. (eds.)].

[2] Höök, M., and Tang, X., 2013, "Depletion of Fossil Fuels and Anthropogenic Climate Change—A Review," Energy Policy, **52**, pp. 797–809.

[3] Lefevre, N., 2010, "Measuring the Energy Security Implications of Fossil Fuel Resource Concentration," Energy Policy, **38**(4), pp. 1635–1645.

[4] Healy, N., and Barry, J., 2017, "Politicizing Energy Justice and Energy System Transitions: Fossil Fuel Divestment and a "Just Transition"," Energy Policy, **108**, pp. 451–459.

[5] Enshaee, A., and Enshaee, P., 2017, "Transmission Loss Allocation Based on Power Adjacency Matrix in Pool Electricity Markets," J. Energy Eng., **143**(2), p. 04016049.

[6] Takebayashi, H., 2015, "Study to Examine the Potential for Solar Energy Utilization Based on the Relationship Between Urban Morphology and Solar Radiation Gain on Building Rooftops and Wall Surfaces," Sol. Energy, **119**, pp. 362–370.

[7] Wani, C., and Gupta, K. K., 2019, "Towards Improving the Performance of Solar Photovoltaic Energy System: A Review," IOP Conf. Ser.: Earth Environ. Sci., **227**, p. 022009.

[8] Genchi, Y., Ishisaki, M., Ohashi, Y., Kikegawa, Y., Takahashi, H., and Inaba, A., 2003, "Impacts of Large-Scale Photovoltaic Panel Installation on the Heat Island Effect in Tokyo," Reprints of the 5th International Conference on Urban Climate, Lodz, Poland, Sept. 1–5.

[9] Golden, J. S., Carlson, J., Kaloush, K. E., and Phelan, P., 2007, "A Comparative Study of the Thermal and Radiative Impacts of Photovoltaic Canopies on Pavement Surface Temperatures," Sol. Energy, **81**(7), pp. 872–883.

[10] Masson, V., Bonhomme, M., Salagnac, J.-L., Briottet, X., and Lemonsu, A., 2014, "Solar Panels Reduce Both Global Warming and Urban Heat Island," Front. Environ. Sci., **2**, p. 14.

[11] Salamanca, F., Georgescu, M., Mahalov, A., Moustaoui, M., and Martilli, A., 2016, "Citywide Impacts of Cool Roof and Rooftop Solar Photovoltaic Deployment on Near-Surface Air Temperature and Cooling Energy Demand," Boundary Layer Meteorol., **161**(1), pp. 203–221.

[12] Taha, H., 2013, "The Potential for Air-Temperature Impact From Large-Scale Deployment of Solar Photovoltaic Arrays in Urban Areas," Sol. Energy, **91**, pp. 358–367.

[13] Pham, J. V., Baniassadi, A., Brown, K. E., Heusinger, J., and Sailor, D. J., 2019, Comparing Photovoltaic and Reflective Shade Surfaces in the Urban Environment: Effects on Surface Sensible Heat Flux and Pedestrian Thermal Comfort, Urban Clim., 29, p. 100500.

[14] Scherba, A., Sailor, D. J., Rosenstiel, T. N., and Wamser, C. C., 2011, "Modeling Impacts of Roof Reflectivity, Integrated Photovoltaic Panels and Green Roof Systems on Sensible Heat Flux Into the Urban Environment," Build. Environ., **46**(12), pp. 2542–2551.

[15] Dominguez, A., Kleissl, J., and Luvall, J. C., 2011, "Effects of Solar Photovoltaic Panels on Roof Heat Transfer," Sol. Energy, **85**(9), pp. 2244–2255.

[16] Miller, W. A., Brown, E., and Livezey, R. J., 2004, "Building-Integrated Photovoltaics for Low-Slope Commercial Roofs," ASME J. Sol. Energy Eng., **127**(3), pp. 307–313.

[17] Wang, Y., Tian, W., Ren, J., Zhu, L., and Wang, Q., 2006, "Influence of a Building's Integrated-Photovoltaics on Heating and Cooling Loads," Appl. Energy, **83**(9), pp. 989–1003.

[18] Wang, Y., Wang, D., and Liu, Y., 2017, "Study on Comprehensive Energy-Saving of Shading and Photovoltaics of Roof Added PV Module," Energy Procedia, **132**, pp. 598–603.

[19] Yang, H., Zhu, Z., Burnett, J., and Lu, L., 2001, *A Simulation Study on the Energy Performance of Photovoltaic Roofs*, ASHRAE Transactions. American Society of Heating, Refrigerating and Air Conditioning Engineers, Cincinnati, OH, pp. 129–135.

[20] ASTM, 2012, ASTM Standard, in: G173-03 (Ed.), Standard Tables for Reference Solar Spectral Irradiance: Direct Normal and Hemispherical on 37.

[21] Crawley, D. B., Lawrie, L. K., Winkelmann, F. C., Buhl, W. F., Huang, Y. J., Pedersen, C. O., Strand, R. K., Liesen, R. J., Fisher, D. E., and Witte, M. J., 2001, "EnergyPlus: Creating a New-Generation Building Energy Simulation Program," Energy Build., **33**(4), pp. 319–331.

[22] Witte, M. J., Henninger, R. H., Glazer, J., and Crawley, D. B., 2001, "Testing and Validation of a New Building Energy Simulation Program," Proc. Build. Simul., **2001**, pp. 353–360.

[23] EIA, 2015, *Residential Energy Consumption Survey*, U.S. Department of Energy, Washington, DC.

[24] USCB, 2017, *American Housing Survey*, United States Census Bureau, Washington, DC.

[25] Hendron, R., and Engebrecht, C., 2010, Building America House Simulation Protocols. National Renewable Energy Laboratory Golden, CO. NREL Report/Project Number: TP-550-49426, 79p.

[26] Cort, K. A., and Butner, R. S., 2012, An Analysis of Statewide Adoption Rates of Building Energy Code by Local Jurisdictions. Pacific Northwest National Laboratory Report PNNL-21963, Richland, WA.

[27] DOE, 2017, EnergyPlus Documentation, Engineering Reference, U.S. Department of Energy, Washington, DC, energyplus.net, p. 847

[28] Peng, C., and Yang, J., 2016, "The Effect of Photovoltaic Panels on the Rooftop Temperature in the EnergyPlus Simulation Environment," Int. J. Photoenergy, **2016**, pp. 1–12.

[29] Booten, C., Kruis, N., and Christensen, C., 2012, Identifying and Resolving Issues in Energyplus and DOE-2 Window Heat Transfer Calculations, Final Technical Report, National Renewable Energy Lab Report NREL/TP-5500-55787.

[30] Yazdanian, M., and Klems, J. H., 1993, "Measurement of the Exterior Convective Film Coefficient for Windows in Low-Rise Buildings," ASHRAE Trans., **100**, pp. 1087–1096.

[31] Sleiman, M., Ban-Weiss, G., Gilbert, H. E., Francois, D., Berdahl, P., Kirchstetter, T. W., Destaillats, H., and Levinson, R., 2011, "Soiling of Building Envelope Surfaces and its Effect on Solar Reflectance—Part I: Analysis of Roofing Product Databases," Sol. Energy Mater. Sol. Cells, **95**(12), pp. 3385–3399.

[32] Ortiz, L. E., Gonzalez, J. E., Wu, W., Schoonen, M., Tongue, J., and Bornstein, R., 2018, "New York City Impacts on a Regional Heat Wave," J. Appl. Meteorol. Climatol., **57**(4), pp. 837–851.

[33] Takane, Y., Kikegawa, Y., Hara, M., and Grimmond, C. S. B., 2019, "Urban Warming and Future Air Conditioning Use in an Asian Megacity: Importance of Positive Feedback," npj Clim. Atmos. Sci., **2**(1), pp. 1–11.